Surface Quality of Fe, Ni, and Cr added Hyper-eutectic Al-Si Automotive Alloys under Up-milling and Down-milling Operation

Akib Abdullah Khan[1], Mashiur Rahman Shoummo[1], Mohammad Salim Kaiser[2*]

[1]Department of Mechanical Engineering, Bangladesh University of Engineering and Technology, Dhaka-1000, Bangladesh
[2]Directorate of Advisory, Extension and Research Services, Bangladesh University of Engineering and Technology, Dhaka-1000, Bangladesh
*Corresponding author: mskaiser@iat.buet.ac.bd

ABSTRACT

Effect of the elements Fe, Ni, and Cr on the surface quality under machining of hyper-eutectic aluminium-based Al-Si automotive alloys has been carried out as the elements improve the properties of this alloy. Machining is done on a horizontal type milling machine using a high-speed steel slab milling cutter in dry condition. Only the cutting speed varies throughout the experiment, while the machining feed and depth of cut remain fixed. The experimental results show that the addition of these alloying elements increases the roughness and hardness specially due to formation of Fe-rich intermetallic $\beta-Al_5FeSi$. However, the needle-like $\beta-Al_5FeSi$ has been refined with the addition of Cr, as seen by the microstructure. The SEM fractography shows a huge cleavage of the brittle $\beta-Al_5FeSi$ phase, which initiates the crack propagation for Fe added alloys. The downward force causes compressive stress exerted in down-milling operation, so the results depict higher hardness and better surface finish. Besides, shorter chips are formed in down-milling than up-milling process, which rather causes the brittleness of the alloys. When the cutting speed is raised, the surface quality deteriorates due to high temperature, while the hardness improves initially due to formation of precipitates then decreases due to coarsening of precipitates.

Copyright © 2022. Journal of Mechanical Engineering Science and Technology.

Keywords: Chips, hardness, microstructure, roughness, surface

I. Introduction

Al-Si alloys are used to manufacture connecting rods, pistons, cylinder liners, engine blocks, etc., components of engine construction in automotive applications, as they are light in weight and have high strength [1]-[5]. To develop the diverse properties of this alloy, several other components are added. When minor elements Cu and Mg are alloyed, it improves the involuntary properties. Moreover, the alloy offers the quick response to heat treatment [4], [5]. Iron is found in aluminum as the most common impurity. Small amount of iron into pure alloys provides slightly higher strength [6], [7]. The addition of Ni effectively increases the properties associated with the elevated temperature of the Al-Si alloy. A number of complex thermally stable intermetallic are formed, which enhance the mechanical properties of the alloys, especially at higher temperatures ahead of 250 °C [8], [9]. The acceptance of higher amount of Fe in Al-Si alloy can be effectively enhanced by adding Ni [10]. Chromium is alloyed to aluminium alloys for controlling the grain structure, preventing the grain growth and to slow down the recrystallization during heat treatment. Chromium reduces aluminum susceptibility and stress corrosion improving the toughness

property [11]. Iron forms intermetallic phases, which are brittle and hard, so the amount of iron in Al-Si alloys should not be high. Addition of adapt elements such as manganese, nickel, zinc, lead, vanadium, chromium, magnesium, copper etc. modifies the morphology of the harmful platelet iron intermetallic compounds to harmless shapes [10]-[12]. The inclusion of Cr accelerates the transformation of Fe-containing phases from β-AlFeSi to α-Al(Fe,Cr)Si. β-AlFeSi has a needle-like shape, while α-Al(Fe,Cr)Si has a fishbone-like morphology [13]. A brief literature review also has been made on the morphological change of different aluminum alloys under machining [14].

However, for manufacturing or repairing the final product, the alloy is machined using several methods and machine tools to produce the desired shape. It can also be observed that the internal structure of the alloys is dramatically affected by the machinability [15]. This structure can be modified through adding alloying elements, process selection, or heat treating subsequently [15]. One of the methods of machining is milling, which is done on milling machines. Milling is a machining operation that removes material from a workpiece by combining the rotation of a multiple-point cutting tool with the advancement (or feeding) of the workpiece at an angle to the tool's axis [16]. Milling can be divided into two types: traditional (or up) milling and climb (or down) milling. The relationship between the cutter's rotation and the feed direction is the distinction between these two approaches. "Up-milling" is when the cutter rotates in the opposite direction of the workpiece, while "down-milling" is when the cutter rotates in the same direction as the workpiece. This machining method affects various properties of the surface being machined. Experimental studies reveal that the quality of the machined surface not only depends on the cutting parameters applied but also the composition and conditions of the alloy samples [17]-[19].

As there is little information in the literature, this study is to find out the effect of the alloying elements like Fe, Ni, and Cr on the machinability using milling machine in terms of roughness, hardness, chips formation, surface quality and microstructural observation of the automotive Al-Si alloys. A comparison also has been made between both the processes of up-milling and down-milling.

II. Material and Methods

A 390 grade aluminium engine block was melted as master alloy. No alloying element was added to the first alloy. Then some Fe was added while casting the second alloy. Ni and Cr were further added to cast the third and fourth alloys, respectively. The prepared alloys are analysed by spectrochemical methods, as shown in Table 1.

Table 1. Values of wt.% composition for the experimental alloys

Alloy	Si	Fe	Ni	Cr	Cu	Mg	Zn	Mn	Ti	Al
1	19.209	0.795	0.089	0.040	2.826	0.245	1.117	0.214	0.099	Bal
2	17.947	**5.910**	0.091	0.086	2.881	0.186	1.139	0.183	0.071	Bal
3	18.913	**6.256**	**0.567**	0.057	2.889	0.193	1.124	0.178	0.090	Bal
4	19.363	**5.501**	**0.621**	**1.267**	3.112	0.232	1.085	0.217	0.076	Bal

The melting was carried out in a ceramic fiber type laboratory-scale resistance heating furnace where degasser and borax were used as suitable flux cover. The chamber of the furnace was sized at $450 \times 450 \times 450$ millimeters with a maximum working temperature of

930 °C. Four heats were taken to develop an Al-Si-based alloy for engine construction. The master alloy was remelted to prepare Alloy 1. Then, to prepare Alloy 2, which mainly contained Fe, mild steel chips were added to the master alloy. Next, chips created from mild steel and some Ni were added to prepare Alloy 3, which mainly contained Fe and Ni. Finally, Alloy 4 was developed through the some stainless-steel chips addition in to the master alloy to full fill the requirement of the level of Fe and Ni along with Cr. For casting, the furnace temperature was always maintained at 750±15 °C with the help of electronic controller. Iron metal moulds were preheated to 200 °C, and casting was done into them. Mould sizes were $20 \times 150 \times 300$ millimeters. The cast alloy was kept in a muffle furnace at 400 °C for 18 hours of homogenization and was air-cooled. Afterward, the homogenized samples were solutionized at 530 °C for 2 hours, and then the samples were salt ice water quenched to get a supersaturated single-phase region. Next, the alloys were isothermally aged at 175 °C for 240 minutes, as the peak hardness of the alloys is achieved at that condition [19], [20]. The samples were wet sanded mechanically with SiC papers of 120, 320, and 1200 grit. The machining operation was done with an HSS (high-speed steel) slab milling cutter mounted on a horizontal milling machine on $300 \times 50 \times 20$ millimeters bars of the four alloys. The experimental setup is shown in Figure 1. The feed was 9.5 mm and kept constant throughout the experiment. Machining parameters, including cutting speed, feed rate, and depth of cut are crucial in terms of the workpiece's process-structure-performance relationship, so they must be chosen carefully [21]. So, the experiment was carried out by varying the cutting speed without the influence of any cutting fluids. The cutter was frequently being cleaned with a brush during the milling operation so that chips were removed from the cutter, which was spoiling the machined surface. A Tylor Hubson surface roughness tester was used to measure surface roughness. An average of five measurements was taken to calculate roughness. A Zwick Rockwell hardness tester with 1/8 inch ball was used to get hardness values in the B scale. A USB microscope was used for observing the machined surfaces, and a DSLR camera was used to capture digital photographs of the generated chips. Table 2 shows the tool geometry and cutting conditions used in the experiment. The specimens were polished with alumina and etched with Keller's reagent for scanning electron microscopy as well as fractographic observations of the surfaces of the alloys using the Jeol Scanning Electron Microscope JSM-5200.
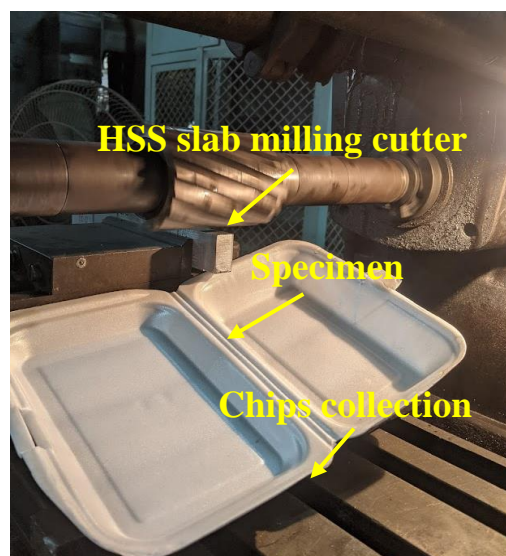

Fig. 1. Experimental setup.

Table 2. Tool geometry and cutting condition.

Cutter Diameter	76.2 mm
Cutter Height	101.6 mm
Cutter Helix Angle	20°
Cutter Rake Angle	8°
Cutter Teeth	16 no.
Feed	9.5 mm/min
Depth of Cut	1.0 mm
Cutting Speed	7.9, 12.9, 14.8, 18.9, 23.9 m/min
Cutting Condition	Dry

III. Results and Discussions

A. Surface Roughness

Surface roughness variation with the cutting speed of the cast and aged hypereutectic different experimental Al-Si automotive alloys is shown in Figures 2 and 3 under up-milling and down-milling machining processes, respectively. From both figures, it can be noted that base Alloy 1 be evidence for lower roughness, whereas Fe added Alloy 2 has rougher surface, and the roughness increases accordingly as Ni and Cr are added too. Common needle-like $\beta-Al_5FeSi$ intermetallic phases are formed due to the presence of Fe in the hypereutectic based alloys, which strongly degrades the mechanical and physical properties of Alloy 2 and 3. Because intermetallic compounds are brittle and rigid, they can operate as stress raisers and sources of weakness, reducing the alloy's strength and ductility. In the alloy matrix, the compounds behave as distinct particles having a highly faceted character. As a result, it has a poor bonding within the matrix, resulting in the lowest impact strength [22]. When the cutter in a milling machine is worked upon, these needle-like brittle intermetallic compounds break down into smaller particles, resulting in an uneven surface finish. It can be seen that when Ni is added, AlSiFeNi and Chinese script intermetallics develop. According to the Ni content, these intermetallic structures are more common in Al dendrites [23]. These intermetallics are long needle-like, making the alloy more prone to blow-holes and porosity. As a result, the bond strength with the matrix is lower, resulting in a rougher surface. When Cr is added, the morphology of the platelet iron intermetallic complex changes to innocuous forms, improving the mechanical capabilities but lowering the surface quality [11], [23]. An earlier investigator has discovered a similar result in Cr added Al-Si alloy with 0.52 wt% Fe [24]. The intermetallic compound is broken down into tiny bits and disseminated throughout the matrix [23].

An interesting fact can be observed from the figures that the surface quality of down-milled surfaces is superior than that of up-milled surfaces. The cause for this could be Al has a tendency to form the built-up edge through the attachment with cutting tool during machining. It has an unfavorable outcome on the surface finish, making it undesirable [24], [25]. During up-milling, the cutter applies outward force to the material, shearing it and increasing BUE. Down-milling, on the other hand, exerts an inward force on the alloy, compressing it and smoothing the surface. From Figures 2 and 3, it is also evident that the surface quality reduces while the cutting speed is gradually increased. Increase in cutting speed increases the surface temperature, and at high temperature grains are coarsed, the

intermetallics are broken into pieces and brittle state of the intermetallics appears at the surface, creating rougher surface. The heat is generated by the friction between the cutting tool and workpiece interface during chip removal since it raises the temperature in the cutting zone which reduces the cutting tool material's hardness [26]. Many studies have found that as the cutting tool hardness decreases, the wear of cutting tool goes faster, changing the cutting edge and shape of the broken chip. As a result, this wear has an undesirable effect on surface roughness and dimensional accuracy [26], [27].
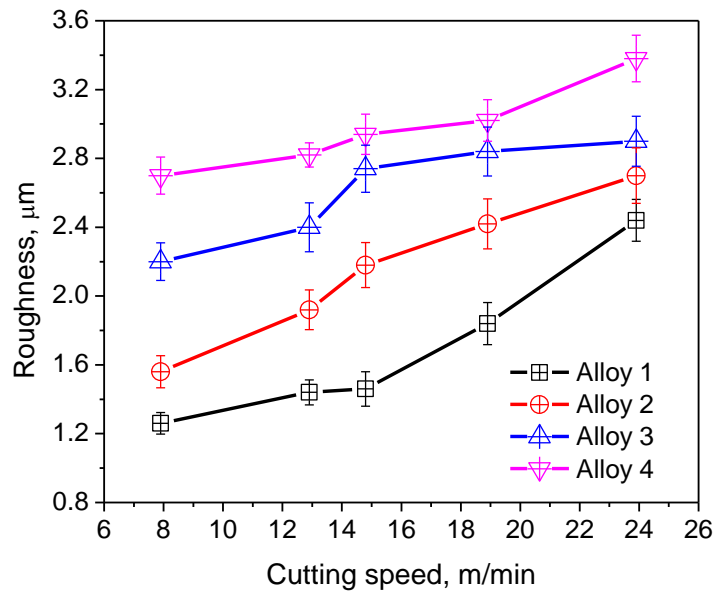
Fig. 2. Surface roughness variation with cutting speed of the experimental alloys under up-milling process.
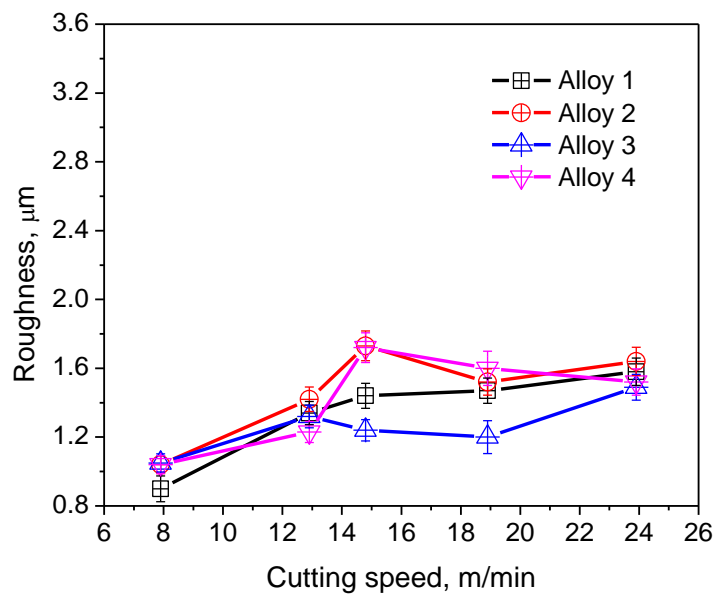

Fig. 3. Surface roughness variation with cutting speed of the experimental alloys under down-milling process.

B. Hardness

Figures 4 and 5 show the hardness of the machined surfaces of the experimental alloys for up-milling and down-milling operations at various cutting speeds. It is clear that Alloys 2, 3, and 4 have higher hardness ratings than Alloy 1. The higher amount of Fe produced iron rich intermetallic during solidification and ageing, which increases the hardness of the alloys [27]. There are the five main Fe-rich phases: $Al_3Fe, \alpha - Al_8Fe_2Si, \beta - Al_5FeSi, \delta - Al_4FeSi_2$ and $\gamma - Al_3FeSi$. Among them, $\beta - Al_5FeSi$ phase is usually accountable for the higher hardness. It can be seen that the same intermetallics which are responsible for degrading surface quality are also responsible for improving hardness rating. Alloy 3 shows a further improvement of the hardness. Adding Ni after age hardening increases the hardness, which could be related to the development of harder precipitated phases such as Ni_3Al and Ni_3Si during the aging process [28], [29]. Conversely, Cr alters the morphology and type of Fe-rich intermetallic phases in cast aluminum alloys, resulting in a loss of hardness in Alloy 4 [11].

However, another intriguing finding is that down-milling produces superior quality in terms of hardness than up-milling. The reason for this could be that when down-milling, the cutter provides compressive force, which is similar to cold rolling, and cold rolling improves hardness by reducing defects such as pinholes and porosity, and increasing dislocation density [30].
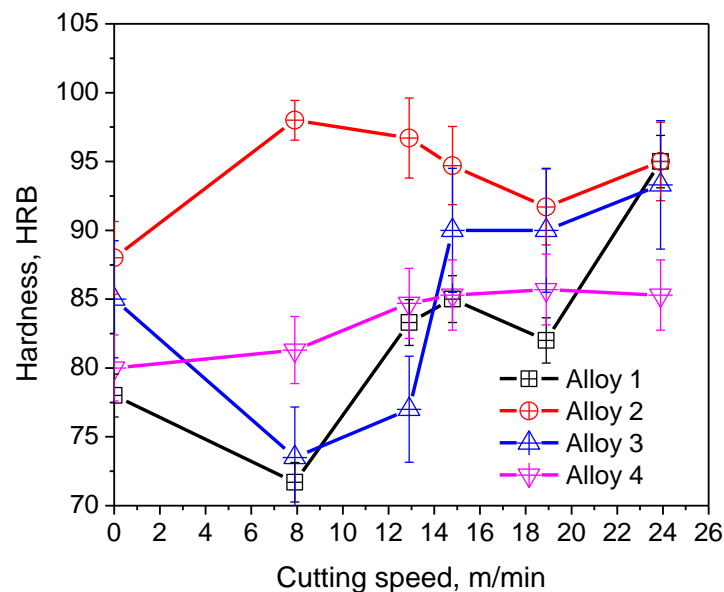

Fig. 4. Rockwell hardness variation with cutting speed of the experimental alloys under up-milling process.

Figures 4 and 5 depict again that the Rockwell hardness number increases as cutting speed is raised up to a certain speed, then the hardness starts to fall again. The surface temperature rises as the speed of the cutter increases, and after a certain point, the precipitates grow coarser, and coarse precipitates are less effective at resisting dislocation movement than finely dispersed precipitates. It is possible that the softening of the alloys at higher temperatures is related to particle coarsening. It can be seen from Figures 2 to 5 that the surface roughness and hardness variation with cutting speed are opposite to each other.

As the speed is increased, the surface roughness rises, whereas the hardness is improved. Previous research suggests that the harder the ductile material, the higher the surface roughness values. However, in the case of brittle material, it was discovered that the variation was very closer between them. It was also stated that the porous-like defects into the alloy play a significant task on machinability of brittle materials, with the higher level of porous material recording higher roughness values owing to such microstructure of the alloy [31].
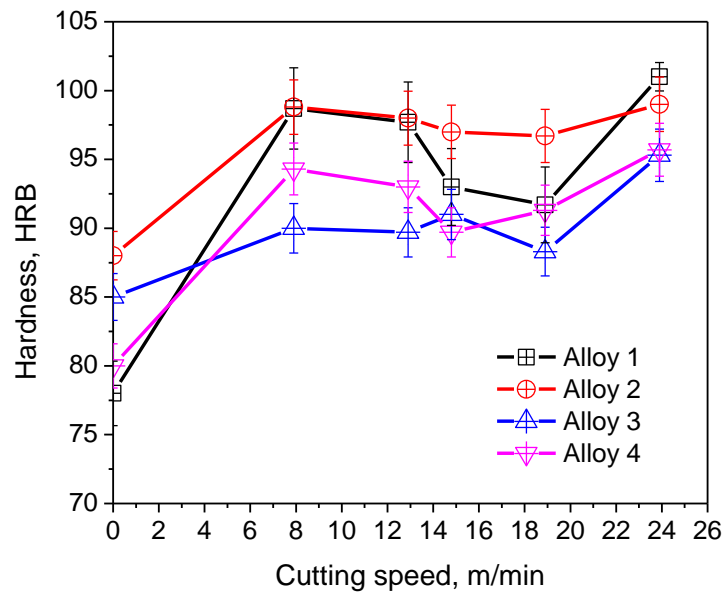

Fig. 5. Rockwell hardness variation with cutting speed of the experimental alloys under down-milling process.

C. Chips Photo Micrographs

Figure 6 shows photomicrographs of chips produced as a result of machining. In the case of up-milling, the chips are longer. Down-milling, on the other hand, results in shorter chips. When down-milling, a compressive force is applied to the surface, and due to high amount of force, the bonds between molecules are frequently broken. As a result, the chips are shattered during down-milling and got shorter in length. The chip size decreases from Figures 6(a) to 6(c) for up-milling and from 6(e) to 6(g) for down-milling. As previously discussed, the intermetallics which are formed due to alloy addition are responsible for this result. As intermetallic compounds with Fe and Ni are formed, the alloys become more brittle. The intermetallics are broken into pieces as machining force is applied and are dispersed throughout the material and the surface. Thus, the mechanical property decreases [21], [22]. Hence, the chips are broken in short segments. On the other hand, from Figure 6(d) for up-milling and Figure 6(h) for down-milling, it is noticeable that the chips are rather longer relatively. When Cr is added, however, the morphology of the intermetallic compound changes to a more favorable state, improving mechanical properties [11], [23].
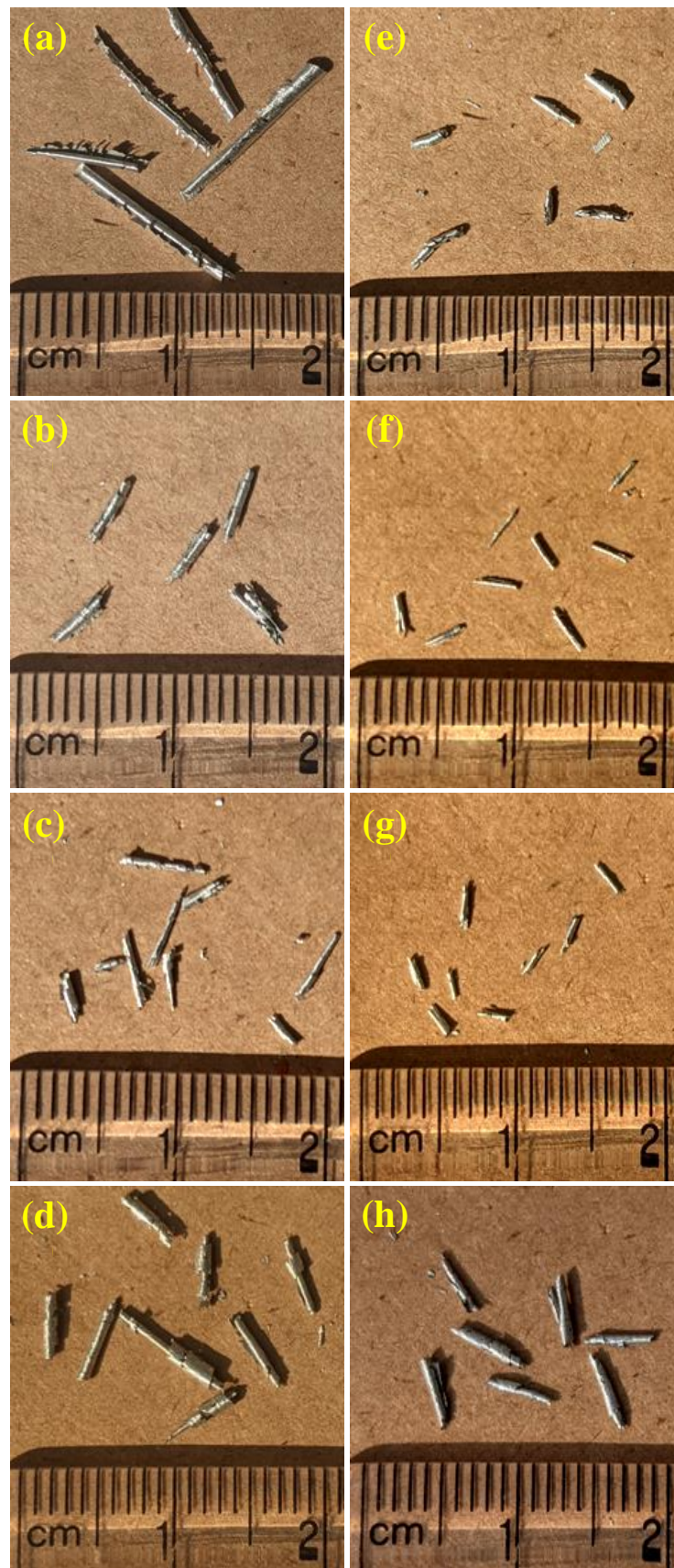
Fig. 6. Optical images of the machined chips at cutting speed 23.9 m/min and depth of cut 1 mm, under up-milling (a) Alloy 1 (b) Alloy 2 (c) Alloy 3 (d) Alloy 4 and under down-milling (e) Alloy 1 (f) Alloy 2 (g) Alloy 3 (h) Alloy 4.

D. Microstructural Observations

Before machining, polished surfaces are smooth, and no plastic deformation is observed on the surface, which can be seen from the optical images in Figure 7. Much information cannot be extracted from this type of optical micrographs. However, for polished surfaces of Alloy 1 to 4, as alloying elements (Fe, Ni, Cr) are added, the tone becomes slightly different. The variation in the amount of elements present into the alloys is responsible for some variation in terms of different levels of tones in different alloys. The similar variation of tone was observed in previous studies of Al-Si alloy, too [32].
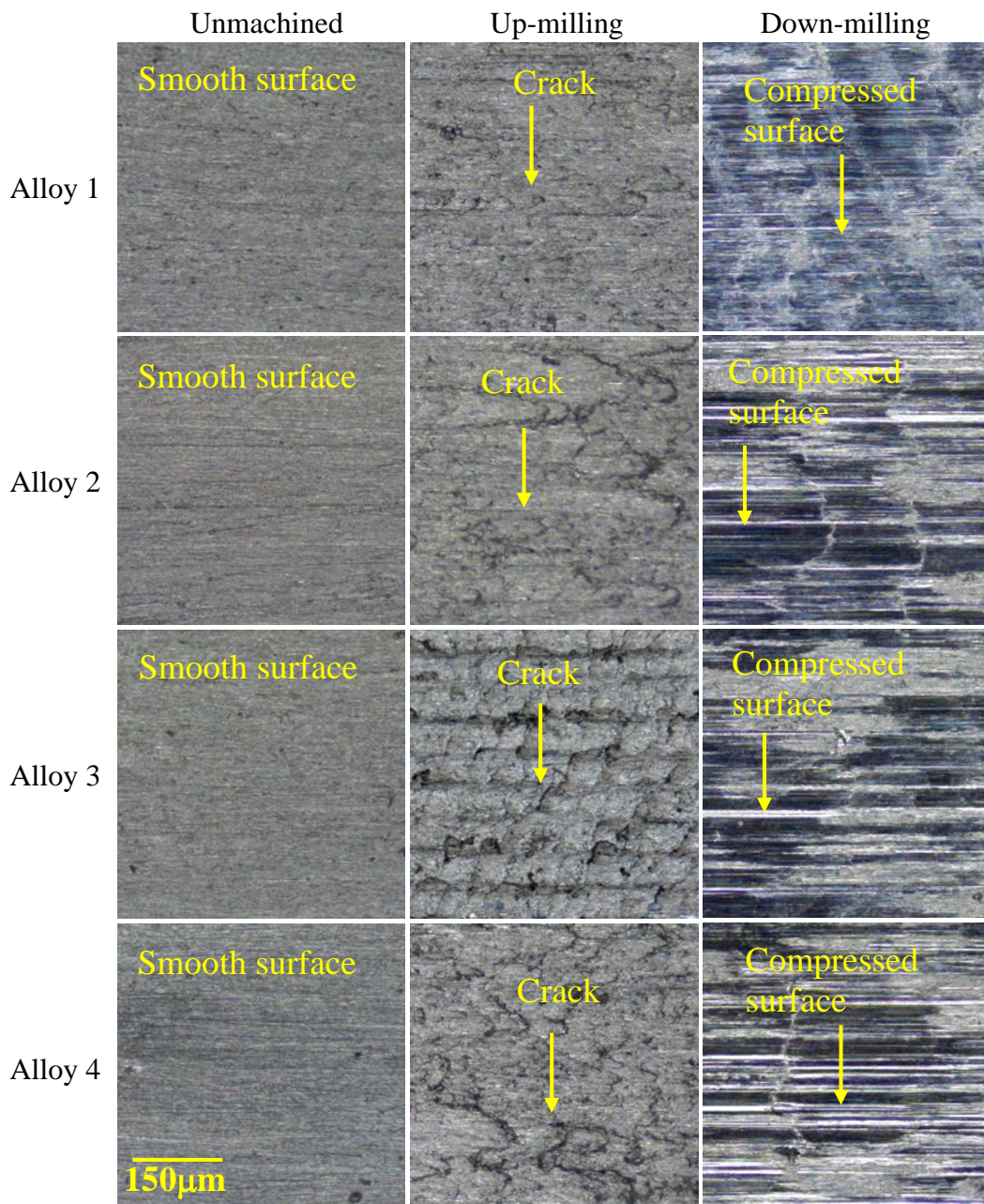

Fig. 7. Optical images of the machined surface at cutting speed 23.9 m/min and depth of cut 1 mm of the experimental alloys under up-milling and down-milling conditions.

After machining under up-milling condition, the micrographs consist of different cracks and more uneven surfaces than those created by down-milling. It is due to the tensile shear occurring during up-milling operation. Micrograph of Alloy 1 displays relatively the minimum cracks on the surface. But Fe added Alloy 2 shows more cracks due to presence of higher level of Fe-rich intermetallic followed by Fe and Ni added Alloy 3 which is due to both Fe and Ni rich needle-like intermetallics. However, Cr Added Alloy 4 can reduce this phenomenon by changing the morphology of Fe-rich intermetallic phases [11], [23]. In case of down-milling operation, lower cracks and pinholes are observed due to compressive stress, which occurs like cold rolling. On the other hand, the uneven surfaces are produced similarly as up-milling operation, but in different intensity, due to presence of different hard intermetallics.

E. Scanning Electron Microscopy

The SEM in Figure 8 shows the microstructure of experimental automotive alloys at peak aged condition. The microstructures as usual consist of primary Al dendrites with eutectic Si phases and a number of intermetallic phases in the matrix. Mixtures of intermetallic compounds are formed in the matrix due to the presence of Fe, Ni, Cr, Cu, and Mg in the alloys. Platelets and acicular morphologies can be seen in eutectic Si particles. Voids and hollow space can be noticed in the microstructure as a casting defect of cast alloys [28].
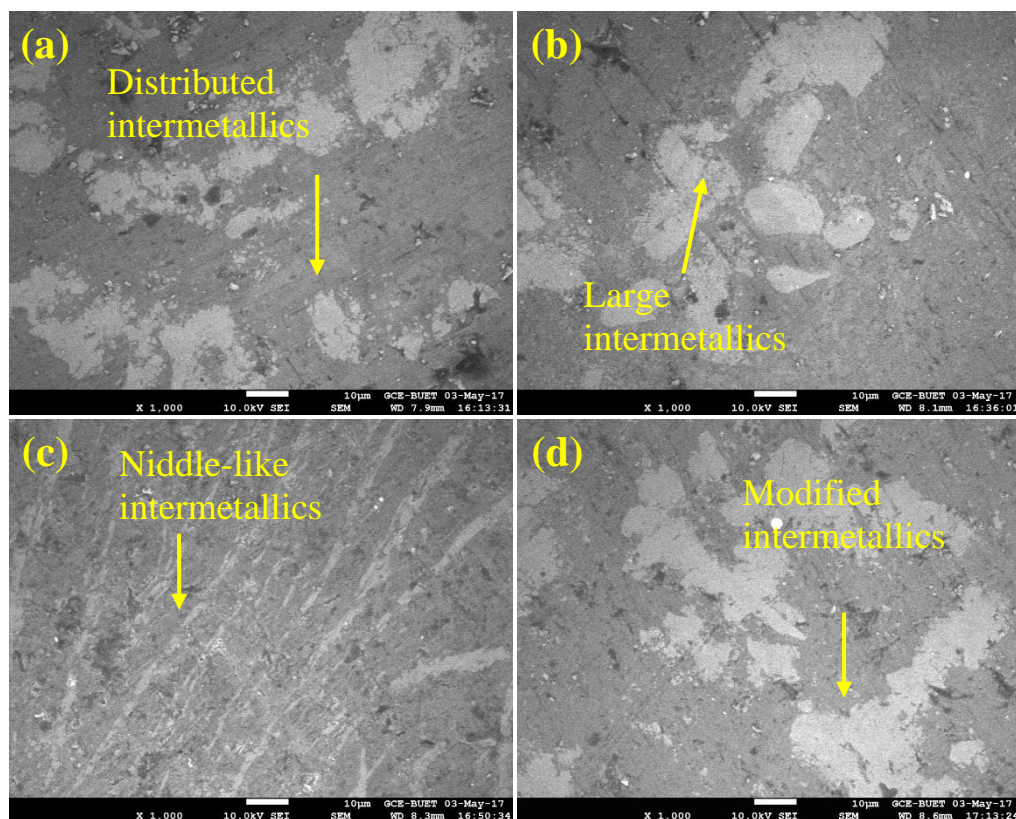

Fig. 8. SEM images of the peak aged (a) Alloy 1, (b) Alloy 2, (c) Alloy 3, and (d) Alloy 4.

The microstructure in Figure 8(a) shows of the base alloy as it contains 0.85 wt% Fe. As the percentage of iron is low, it has a small amount of $\beta - Al_5FeSi$ phase, which can be

witnessed in Figure 8(a). Figure 8(b) shows that the microstructure of Fe accompanying Alloy 2 has a higher amount of $\beta - Al_5FeSi$ phase than Alloy 1 in Figure 8(a) due to the excess Fe in the alloy. Because Alloy 3 contains a considerable quantity of Ni, there are two types of Al_3Ni phases: plate-like and needle-like. The long needle-like structures can be seen in Figure 8(c), which covers most of the area. As previously discussed, these structures are responsible for blow-holes, pinholes, and porosity, which again is responsible for the degraded quality of surface. Figure 8(d) shows SEM micrographs of Cr-added Alloy 4, which has a changed structure with plate-like and needle-like morphologies missing.

Figure 9 shows the SEM fractographs of the tensile tested peak aged alloys. The SEM fractograph of Alloy 1 is shown in Figure 9(a), which indicates a cleavage fracture. It occurs due to the high deformation rates during loading. Every grain has different orientation of the fracture plane. As secondary cracks, intergranular cleavage is visible too. Crack initiation occurs by significant cleavage of the brittle $\beta - Al_5FeSi$ phase, according to the SEM fractograph of Alloy 2 (Figure 9(b)). At such Fe levels, a proliferation of β-platelets is expected in the alloy microstructure. The crack propagates from one β-platelet to the next, which can be seen in the Figure 9(b). In comparison to Si particles, the plate-like $\beta - Al_5FeSi$ phase has substantially greater dimensions, making it more vulnerable to crack initiation. Increased number of secondary cracks is visible in Figure 9(c), because during age-hardening, the alloy becomes more brittle due to more precipitation hardening of the Ni-rich phases. As Cr changes, the $\beta - Al_5FeSi$ phases in the alloy, no cracks propagating between the matrix and β-particles are detected in the SEM picture of Alloy 4 (Figure 9(d)) [33].
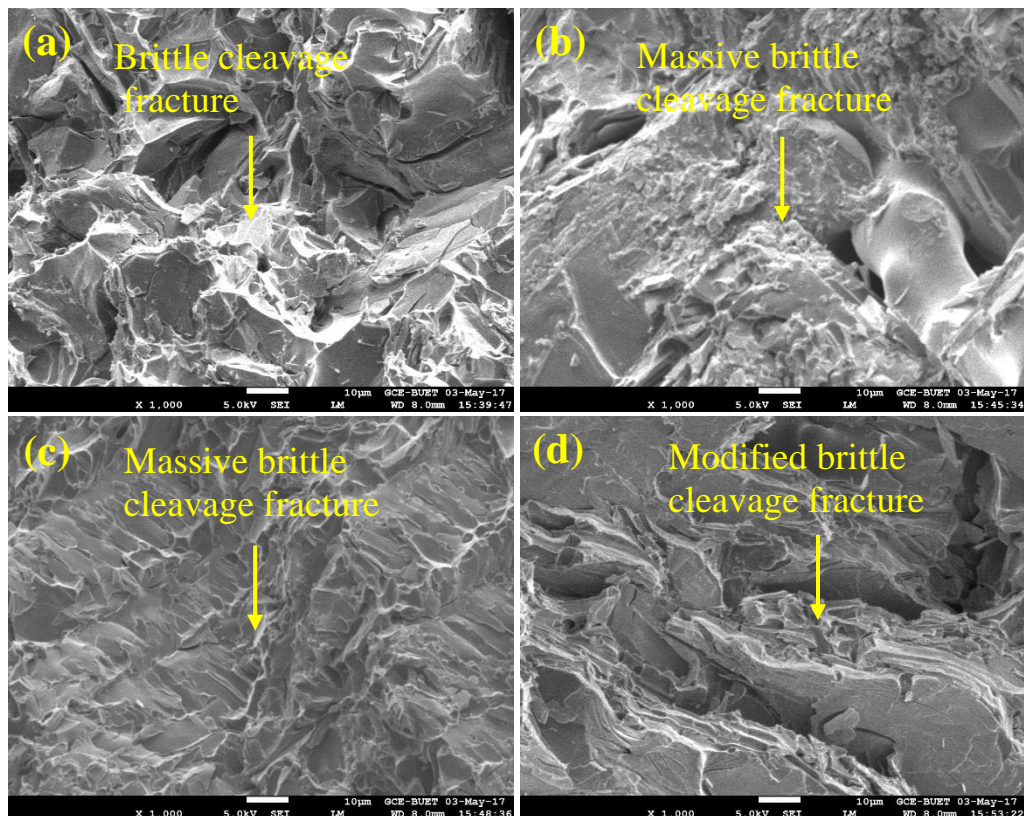

Fig. 9. SEM fractograph of peak aged (a) Alloy 1, (b) Alloy 2, (c) Alloy 3 and (d) Alloy 4.

IV. Conclusion

From this study following results may be concluded regading the alloying elements' effect on the surface quality of discussed Al-Si hyper-eutectic automotive alloy under up-milling and down-milling conditions.

Surface quality degrades as Fe, Ni, and Cr are added in subsequent alloys, because of intermetallic formation as well as creation of porosity and blow holes. The better surface quality and hardness can be achieved through down-milling operation due to compressive force and minimized BUE than for up-milling, acting as tensile-like force. The surface roughness and hardness both are found to be proportional to cutting speed for producing higher temperature at higher speed. The fractured surfaces of Fe and Ni added alloys show more cracks than the base alloy for the formation of different brittle intermetallics, whereas Cr added alloy shows lesser cracks for better morphology of the intermetallic precipitates. The chips produced are shorter in case of down-milling as compressive force acts on the brittle materials unlike of up-milling. The shorter chips are found for Fe and Ni added alloys as increased brittleness, but relatively longer chips are created in case of Cr added alloy due to intermetallic modification.

Acknowledgement

References

[1]   D. K. Dwivedi, "Sliding temperature and wear behaviour of cast Al-Si base alloy," *Mater. Sci. Technol.*, vol. 19, no. 8, pp. 1091–1096, 2003, doi: 10.1179/026708303225004657.

[2]   M. S. Kaiser, M. R. Basher, and A. S. W. Kurny, "Effect of scandium on microstructure and mechanical properties of cast Al-Si-Mg alloy," *J. Mater. Eng. Perform.*, vol. 21, no. 7, pp. 1504–1508, 2012, doi: 10.1007/s11665-011-0057-3.

[3]   C. Subramanian, "Effects of sliding speed on the unlubricated wear behaviour of Al-12.3wt.%Si alloy," *Wear*, vol. 151, no. 1, pp. 97–100, 1991, doi: 10.1016/0043-1648(91)90349-Y.

[4]   K. A. J. Kumar, C. M. Ramesha, M. K. Srinath, and B. Navaneeth, "Fabrication and post processing techniques to enhance the strength of Al-Si alloy," *Mater. Today Proc.*, vol. 59, no. 1, pp. 483–488, 2022, doi: 10.1016/j.matpr.2021.11.470.

[5]   Z. Yang, X. He, B. Li, A. Atrens, X. Yang, and H. Cheng, "Influence of Si, Cu, B, and trace alloying elements on the conductivity of the Al-Si-Cu alloy," *Materials (Basel).*, vol. 15, no. 2, p. 426, 2022, doi: 10.3390/ma15020426.

[6]   T. O. Mbuya, B. O. Odera, and S. P. Ng'ang'a, "Influence of iron on castability and properties of aluminium silicon alloys: literature review," *Int. J. Cast Met. Res.*, vol. 16, no. 5, pp. 451–465, 2003, doi: 10.1080/13640461.2003.11819622.

[7]   K. L. Sahoo and B. N. Pathak, "Solidification behaviour, microstructure and mechanical properties of high Fe-containing Al–Si–V alloys," J. *Mater. Process. Technol.*, vol. 209, no. 2, pp. 798–804, 2009, doi: 10.1016/j.jmatprotec.2008.02.043.

[8]   F. Stadler, H. Antrekowitsch, W. Fragner, H. Kaufmann, and P. J. Uggowitzer, "The effect of Ni on the high-temperature strength of Al-Si cast alloys," *Mater. Sci. Forum*, vol. 690, pp. 274–277, 2011, doi: 10.4028/www.scientific.net/MSF.690.274.

[9]   R. Gholizadeh and S. G. Shabestari, "Investigation of the effects of Ni, Fe, and Mn on the formation of complex intermetallic compounds in Al-Si-Cu-Mg-Ni alloys," *Metall. Mater. Trans. A*, vol. 42, no. November, pp. 3447–3458, 2011, doi: 10.1007/s11661-011-0764-2.

[10] S. A. I. Suhruth, T. Kaja, and P. R. Gangadasari, "Extending the tolerance of iron in cast Al-Si alloy," *JOM*, vol. 73, no. 9, pp. 2652–2657, 2021, doi: 10.1007/s11837-021-04803-x.

[11] A. K. Mukhopadhyay, "Microstructure and properties of high strength aluminium alloys for structural applications," *Trans. Indian Inst. Me*t*.,* vol. 62, no. 2, pp. 113-122, 2009, doi: 10.1007/s12666-009-0015-z.

[12] N. A. Belov, A. A. Aksenov, and D. G. Eskin, *Iron in Aluminium Alloys*, 1st ed. London: CRC Press, 2002.

[13] Y. Yang, S. Y. Zhong, Z. Chen, M. Wang, N. Ma, and H. Wang, "Effect of Cr content and heat-treatment on the high temperature strength of eutectic Al-Si alloys," *J. Alloys Compd.*, vol. 647, pp. 63–69, 2015, doi: 10.1016/j.jallcom.2015.05.167.

[14] M. C. Santos, A. R. Machado, W. F. Sales, M. A. S. Barrozo, and E. O. Ezugwu, "Machining of aluminum alloys: a review," *The International Journal of Advanced Manufacturing Technology*, vol. 86, no. (9-12), pp. 3067-3080, 2016, doi: 10.1007/s00170-016-8431-9.

[15] T. J. Skingle and R. W. Thompson, "Machining of aluminum alloys," *J. Appl. Metalwork.,* vol. 1, no. 2, pp. 76–78, 1980, doi: 10.1007/BF02833612.

[16] A. W. Ronald and R. D. Cormier, *Machining and Metalworking Handbook*, 3rd ed. McGraw-Hill, 2006.

[17] D. K. Dwivedi, A. Sharma, and T. V. Rajan, "Machining of LM13 and LM28 cast aluminium alloys: Part I," *J. Mater. Process. Technol.*, vol. 196, no. 1–3, 2008, doi: 10.1016/j.jmatprotec.2007.05.032.

[18] P. Goel, Z. A. Khan, A. N. Siddiquee, S. Kamaruddin, and R. K. Gupta, "Influence of slab milling process parameters on surface integrity of HSLA: a multi-performance characteristics optimization," *Int. J. Adv. Manuf. Technol.*, vol. 61, no. 9–12, pp. 859–871, 2012, doi: 10.1007/s00170-011-3763-y.

[19] P. A. B. Machado, J. M. do Vale Quaresma, A. Garcia, and C. A. dos Santos, "Investigation on machinability in turning of as-cast and T6 heat-treated Al-(3, 7, 12%) Si-0.6%Mg alloys," *J. Manuf. Process.*, vol. 75, pp. 514–526, 2022, doi: 10.1016/j.jmapro.2022.01.028.

[20] M. S. Kaiser, "Solution Treatment Effect on Tensile, Impact and Fracture Behaviour of Trace Zr Added Al–12Si–1Mg–1Cu Piston Alloy," *J. Inst. Eng. Ser. D,* vol. 99, no. 1, pp. 109–114, 2018, doi: 10.1007/s40033-017-0140-5.

[21] M. C. Shaw, "*Metal Cutting Principles*," New York: Oxford University Press, 2005, p. 672.

[22] S. G. Shabestari, "The effect of iron and manganese on the formation of intermetallic compounds in aluminum–silicon alloys," *Mater. Sci. Eng. A*, vol. 383, no. 2, pp. 289–298, 2004, doi: 10.1016/j.msea.2004.06.022.

[23] D. Ozyurek, M. Yıldırım, B. Yavuzer, I. Simsek, and T. Tuncay, "The effect of Ni addition on microstructure and mechanical properties of cast A356 alloy modified with Sr," *Met. Mater.*, vol. 59, no. 06, pp. 391–399, 2021, doi: 10.4149/km_2021_6_391.

[24] G. Gustafsson, T. Thorvaldsson, and G. L. Dunlop, "The influence of Fe and Cr on the microstructure of cast Al-Si-Mg alloys," *Metall. Trans. A*, vol. 17, no. 1, pp. 45–52, 1986, doi: 10.1007/BF02644441.

[25] S. Gangopadhyay, R. Acharya, A. K. Chattopadhyay, and V. G. Sargade, "Effect of cutting speed and surface chemistry of cutting tools on the formation of bul or bue and surface quality of the generated surface in dry turning of AA6005 aluminium alloy," *Mach. Sci. Technol.*, vol. 14, no. 2, pp. 208–223, 2010, doi: 10.1080/10910344.2010.500961.

[26] O. Özbek and H. Saruhan, "The effect of vibration and cutting zone temperature on surface roughness and tool wear in eco-friendly MQL turning of AISI D2," *J. Mater. Res. Technol.*, vol. 9, no. 3, pp. 2762–2772, 2020, doi: 10.1016/j.jmrt.2020.01.010.

[27] W. Bai, A. Roy, R. Sun, and V. V. Silberschmidt, "Enhanced machinability of SiC-reinforced metal-matrix composite with hybrid turning," *J. Mater. Process. Technol.*, vol. 268, no. August 2018, pp. 149–161, 2019, doi: 10.1016/j.jmatprotec.2019.01.017.

[28] M. S. Kaiser, S. H. Sabbir, M. S. Kabir, M. R. Soummo, and M. Al Nur, "Study of mechanical and wear behaviour of hyper-eutectic Al-Si automotive alloy through Fe, Ni and Cr addition," *Mater. Res.*, vol. 21, no. 4, 2018, doi: 10.1590/1980-5373-mr-2017-1096.

[29] S. Ji, W. Yang, F. Gao, D. Watson, and Z. Fan, "Effect of iron on the microstructure and mechanical property of Al–Mg–Si–Mn and Al–Mg–Si die cast alloys," *Mater. Sci. Eng. A*, vol. 564, pp. 130–139, 2013, doi: 10.1016/j.msea.2012.11.095.

[30] R. Mittal and D. Singh, "Effect of cold rolling on the mechanical properties of spray cast Al-6Si-20Pb alloy," *Adv. Mater. Res.*, vol. 585, pp. 402–406, 2012, doi: 10.4028/www.scientific.net/AMR.585.402.

[31] N. V Dhandapani, V. S. Thangarasu, and G. Sureshkannan, "Investigation on effect of material hardness in high speed CNC end milling process," *Sci. World J.*, vol. 2015, pp. 1–6, 2015, doi: 10.1155/2015/762604.

[32] M. S. Kaiser, M. R. Qadir, and S. Dutta, "Electrochemical corrosion performance of commercially used aluminium engine block and piston in 0.1M NaCl," *J. Mech. Eng.*, vol. 45, no. 1, pp. 48–52, 2015, doi: 10.3329/jme.v45i1.24384.

[33] M. Mahta, M. Emamy, A. Daman, A. Keyvani, and J. Campbell, "Precipitation of Fe rich intermetallics in Cr- and Co-modified A413 alloy," *Int. J. Cast Met. Res.*, vol. 18, no. 2, pp. 73–79, 2005, doi: 10.1179/136404605225022928.